Hurley, J. B., & Stryer, L. (1982) *J. Biol. Chem. 257*, 11094–11099.
Kalbitzer, H. R., Feuerstein, J., Goody, R. S., & Wittinghofer, A. (1990) *Eur. J. Biochem. 188*, 355–359.
Kanazawa, T., & Tonomura, Y. (1965) *J. Biochem. Tokyo 57*, 604–615.
Kaziro, Y. (1978) *Biochim. Biophys. Acta 505*, 95–127.
Kowalczykowski, S. C. (1987) *Trends Biochem. Sci. 12*, 141–145.
Kuhn, H., Bennett, N., Michel-Villaz, M., & Chabre, M. (1981) *Proc. Natl. Acad. Sci. U.S.A. 78*, 6873–6877.
Liebman, P. A., & Pugh, E. N., Jr. (1980) *Nature (London) 287*, 734–736.
Liebman, P. A., Park, K. R., & Dratz, E. A. (1987) *Annu. Rev. Physiol. 49*, 765–791.
McCormick, F. (1989) *Cell 56*, 5–8.
Melki, R., Carlier, M.-F., & Pantaloni, D. (1990) *Biochemistry 29*, 8921–8932.
Menon, A. S., Waxman, L., & Goldberg, A. L. (1987) *J. Biol. Chem. 262*, 722–726.
Navon, S. E., & Fung, B. K.-K. (1984) *J. Biol. Chem. 259*, 6686–6693.
Pepperberg, D. R., Kahlert, M., Krause, A., & Hofmann, P. K. (1988) *Proc. Natl. Acad. Sci. U.S.A. 85*, 5531–5535.
Porter, M. E., & Johnson, K. A. (1989) *Annu. Rev. Cell Biol. 5*, 119–151.
Roof, D. J., Korenbrot, J. I., & Heuser, J. E. (1982) *J. Cell Biol. 95*, 501–509.
Sitaramayya, A., & Liebman, P. A. (1983a) *J. Biol. Chem. 258*, 1205–1209.
Sitaramayya, A., & Liebman, P. A. (1983b) *J. Biol. Chem. 258*, 12106–12109.
Stryer, L. (1986) *Annu. Rev. Neurosci. 9*, 87–119.
Vallee, R. B., & Shpetner, H. S. (1990) *Annu. Rev. Biochem. 59*, 909–932.
Vuong, T. M., & Chabre, M. (1990) *Nature (London) 346*, 71–74.
Wilden, U., Hall, S. W., & Kuhn, H. (1986a) *Proc. Natl. Acad. Sci. U.S.A. 83*, 1174–1178.
Wilden, U., Wust, E., Weyland, I., & Kuhn, H. (1986b) *FEBS Lett. 207*, 292–295.
Woodruff, M. L., & Fain, G. L. (1982) *J. Gen. Physiol. 80*, 537–555.
Yee, R., & Liebman, P. A. (1978) *J. Biol. Chem. 253*, 8902–8909.

Structure and Interactions of Ether- and Ester-Linked Phosphatidylethanolamines†

Frederick S. Hing, Prakas R. Maulik, and G. Graham Shipley*
Departments of Biophysics and Biochemistry, Boston University School of Medicine, Boston, Massachusetts 02118
Received March 19, 1991; Revised Manuscript Received June 24, 1991

ABSTRACT: The ether-linked phospholipid 1,2-dihexadecylphosphatidylethanolamine (DHPE) was studied as a function of hydration and in fully hydrated mixed phospholipid systems with its ester-linked analogue 1,2-dipalmitoylphosphatidylethanolamine (DPPE). A combination of differential scanning calorimetry (DSC) and X-ray diffraction was used to examine the phase behavior of these lipids. By DSC, from 0 to 10 wt % H_2O, DHPE displayed a single reversible transition that decreased from 95.2 to 78.8 °C and which was shown by X-ray diffraction data to be a direct bilayer gel to inverted hexagonal conversion, $L_\beta \rightarrow H_{II}$. Above 15% H_2O, two reversible transitions were observed which stabilized at 67.1 and 92.3 °C above 19% H_2O. X-ray diffraction data of fully hydrated DHPE confirmed the lower temperature transition to be a bilayer gel to bilayer liquid-crystalline ($L_\beta \rightarrow L_\alpha$) phase transition and the higher temperature transition to be a bilayer liquid-crystalline to inverted hexagonal ($L_\alpha \rightarrow H_{II}$) phase transition. The lamellar repeat distance of gel-state DHPE increased as a function of hydration to a limiting value of 62.5 Å at 19% H_2O (8.6 mol of water/mol of DHPE), which corresponds to the hydration at which the transition temperatures are seen to stabilize by DSC. Electron density profiles of DHPE, in addition to calculations of the lipid layer thickness, confirmed that DHPE in the gel state forms a noninterdigitated bilayer at all hydrations. Fully hydrated mixed phospholipid systems of DHPE and DPPE exhibited two reversible transitions by DSC. X-ray diffraction data of a mixture containing 10 mol % DPPE identified the lower temperature transition as an $L_\beta \rightarrow L_\alpha$ phase transition and the higher temperature transition as an $L_\alpha \rightarrow H_{II}$ phase transition. Addition of DHPE to DPPE slightly increased the $L_\beta \rightarrow L_\alpha$ transition temperature in a linear fashion, suggesting complete miscibility of the L_β and L_α phases. Increasing amounts of DHPE in DPPE decreased by a greater amount the temperature of the $L_\alpha \rightarrow H_{II}$ transition from the extrapolated value in DPPE. The presence of the ether linkage apparently stabilized the L_β and H_{II} phases and destabilized the L_α phase in the mixed DHPE/DPPE system.

The bilayer matrix of plasma cell membranes is comprised of a complex mixture of different glycerol-based and sphingosine-based polar lipids. The appropriate blend of phospholipids, sphingomyelins, and glycosphingolipids, together with cholesterol, apparently assembles to form the stable lipid bilayer which provides both a general permeability barrier and the matrix into which specific functional membrane proteins (channels, receptors, enzymes, etc.) are asymmetrically incorporated. While many individual membrane lipids [e.g., phosphatidylcholine (PC), sphingomyelin, cerebroside, diglycosyldiglyceride (DGDG)] spontaneously assemble to form

† This work was supported by Research Grant HL-26335 and Training Grants HL-07429 and HL-07291 from the National Institutes of Health.
* Address correspondence to this author at the Department of Biophysics, Boston University School of Medicine.

0006-2960/91/0430-9007$02.50/0 © 1991 American Chemical Society

bilayers, others form nonbilayer structures such as the hexagonal (H_{II}) phase [e.g., phosphatidylethanolamine (PE), monoglycosyldiglyceride (MGDG)] or even spherical micelles (gangliosides). In some bacterial membranes, the bilayer/nonbilayer lipid composition is apparently regulated. For example, in *Acholeplasma laidlawii*, the DGDG/MGDG ratio responds to manipulations of the membrane fatty acid composition (Wieslander et al., 1980, 1981a,b); a similar effect has been noted in *Clostridium butyricum* where the ratio of bilayer-forming glycerol acetal PE to hexagonal-preferring PE again responds to alterations in fatty acid composition (Goldfine et al., 1987). Whether these gross structural properties of the individual lipid components are used in regions of membranes responsible for specific functions, e.g., H_{II}-forming lipids in lipid/protein interactions or fusion sites, remains to be established.

Our own work in this field has focused initially on categorizing the structure and properties of membrane polar lipids. For example, we have monitored the effects of variations in polar head-group structure [PE (Chapman et al., 1966; Hitchcock et al., 1974), methylated PEs (Mulukutla & Shipley, 1984), PC (Janiak et al., 1976, 1979; Ruocco & Shipley, 1982a,b), phosphatidylserine (PS: Hauser et al., 1982), etc.] and hydrocarbon chain length, unsaturation, and distribution (Serrallach et al., 1983; Mattai et al., 1987; Shah et al., 1990). While it is clear that variations in both polar group and chain moieties influence lipid structure and properties, recent studies have suggested that alterations in the mode of chain linkage to the glycerol are also important. For example, for PC, substituting ether linkages (alkyl) for ester (acyl) linkages for the attachment of chains at the *sn*-1 and *sn*-2 positions influences both the thermotropic and structural properties. Most striking is the conversion of the usual bilayer gel phase of the ester-linked dipalmitoyl-PC, DPPC, to a chain-interdigitated "monolayer" structure for the ether-linked dihexadecyl-PC, DHPC (Ruocco et al., 1985; Kim et al., 1987a; Laggner et al., 1987). More recently, our studies of 1-hexadecyl-2-palmitoyl-PC (HPPC) demonstrate that substitution at only the *sn*-1 position is sufficient to promote formation of an interdigitated gel phase (Haas et al., 1990). Current studies of its positional isomer (1-palmitoyl-2-hexadecyl-PC, PHPC) should reveal the molecular linkage and perhaps conformational requirements underlying this change in molecular packing (F. S. Hing, R. A. Duclos, and G. G. Shipley, unpublished results). In mixed DPPC/DHPC systems, both types of gel phase are formed (bilayer or interdigitated monolayer) depending on the composition (Kim et al., 1987b; Lohner et al., 1987).

The PEs found in both animal and bacterial membranes often contain significant amounts of PE with chains attached at the *sn*-1 position by ether (or vinyl ether, i.e., plasmalogen) linkages, and minor amounts of dialkylphospholipids are found in some tissues [see Snyder (1985) for a review]. It has been shown that substituting ether for ester linkage lowers the bilayer $L_\alpha \rightarrow H_{II}$ transition temperature but has little effect on the lower gel $\rightarrow L_\alpha$ transition (Boggs et al., 1981; Seddon et al., 1983). Using primarily scanning calorimetry and X-ray diffraction, Seddon and co-workers have provided an excellent picture of the phase behavior of a series of ester- and ether-linked PEs (Seddon et al., 1983, 1984). In the present study, we focus on the hydration dependence of the structure and properties of one member of the ether-linked series, dihexadecyl-PE (DHPE), and then determine its interactions with its ester-linked analogue dipalmitoyl-PE (DPPE). A study of the interactions of the two ether-linked phospholipids, DHPE and DHPC, will be the subject of a separate report (Hing & Shipley, 1991).

Materials and Methods

DHPE Hydration Study. DHPE was obtained from Berchtold (Berne, Switzerland) and purified by column chromatography with Iatrobeads 8060 (Iatron Laboratories, Tokyo, Japan). The DHPE was shown to be >98% pure by thin-layer chromatography (TLC) using the solvent system $CHCl_3/MeOH/H_2O$ (65/25/4 v/v).

Samples for differential scanning calorimetry (DSC) were prepared by weighing anhydrous DHPE into stainless-steel pans. A known aliquot of distilled, deionized water was added, and the pans were sealed and weighed again to determine hydration (expressed as weight percentage of water). DSC was performed on a Perkin-Elmer (Norwalk, CT) DSC-2 calorimeter equipped with a thermal analysis data station (Model 3500). Calorimetry was performed at heating/cooling rates of 5 °C/min over the temperature range 0–98 °C. Samples were heated and cooled at least 3 times to equilibrate. Transition temperatures were determined from the midpoint of the transition peak, and transition enthalpies were determined from the area under the peak. A gallium standard was used to calibrate temperatures and enthalpies. Identification of the phases was made by performing X-ray diffraction of the lipid at a temperature above and below the phase transition. Additional DSC experiments were performed on fully hydrated DHPE and a mixture of DHPE and DPPE with a Microcal-2 calorimeter (Amherst, MA). Aqueous dispersions (5–7 mg/mL) were examined at heating rates of 90 and 10 °C/h.

X-ray diffraction samples were made by weighing DHPE into a 1.0-mm quartz capillary followed by a known amount of distilled, deionized water. Capillaries were then sealed and heated above the chain-melting transition temperature while simultaneously being centrifuged in a clinical centrifuge at high speed. Samples were inverted and centrifuged back and forth in the capillary several times in order to achieve homogeneous mixing. X-ray diffraction patterns were recorded on photographic film using nickel-filtered Cu Kα radiation (λ = 1.5418 Å) from an Elliott GX-6 rotating-anode generator (Elliott Automation, Borehamwood, U.K.) and focused with either double-mirror (Franks, 1958) or toroidal (Elliott, 1965) optics. Microdensitometry was performed on a Joyce Loebl (Gateshead, U.K.) Model III-CS scanning microdensitometer.

Analysis of the structural parameters was performed according to the formalism of Luzzati (1968). From the bilayer periodicity (d), the thickness of the lipid bilayer (d_l), the water layer thickness (d_w), and the area available to one lipid molecule (S) were calculated according to the formulas:

$$d_l = d[1 + (\nu_w/\nu_l)(1 - C)/C]^{-1}$$

$$d_w = d - d_l$$

$$S = 2M_r\nu_l/d_l(N \times 10^{-24})$$

where ν_w and ν_l are the partial specific volumes of water and lipid, respectively, C is the lipid concentration, M_r is the molecular weight of the lipid, and N is Avogadro's number. In calculations of structural parameters, the limiting hydration, as determined from the bilayer periodicity (d), was assumed for those DHPE samples with water contents above this amount.

In order to calculate electron density profiles, the observed lamellar intensities, $I(h)$, were corrected for the Lorentz factor (in our geometry and for unoriented samples, this is proportional to h^2), giving $h^2I(h)$, and each hydration set was nor-

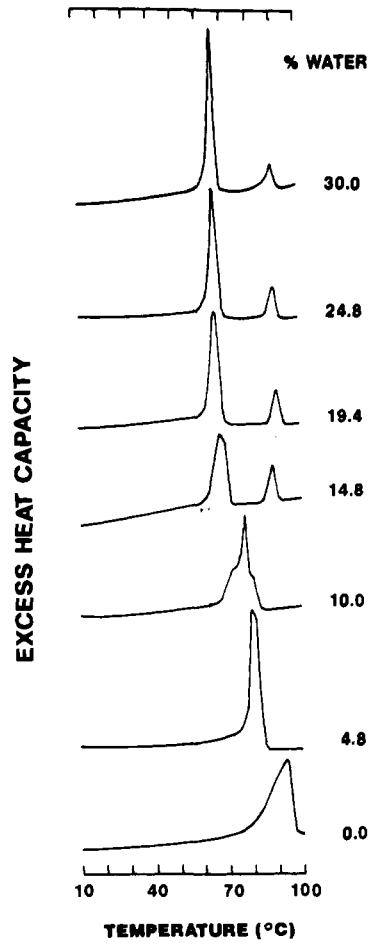

FIGURE 1: Representative DSC heating curves of hydrated DHPE (0.0–30.0 wt % H_2O). Heating rate, 5 °C/min.

malized with respect to each other by using the intensity of the wide-angle reflection at 1/4.18 $Å^{-1}$. The corresponding scaled, normalized structure amplitudes, $F(h)$, are plotted as a function of the reciprocal coordinate s ($s = 2 \sin \theta/\lambda$). Phasing of the lamellar reflections is done by inspection of the plotted amplitude data and by use of the Shannon sampling theorem (Shannon, 1949). The phase combination providing a satisfactory fit to all hydration amplitudes is selected.

DHPE/DPPE Binary Mixtures. DHPE and DPPE (Berchtold, Berne, Switzerland) were found to be >98% pure by TLC in $CHCl_3$/MeOH/H_2O (65/25/4 v/v) and were used without further purification. In order to make DHPE/DPPE mixtures of known molar ratio, appropriate amounts of each lipid were weighed into a small vial and dissolved in chloroform. Solvent was blown off with nitrogen and then evaporated under vacuum overnight. Samples at full hydration (50 wt % H_2O) were prepared for DSC and X-ray diffraction, and examined as described above for pure DHPE samples.

Results

DHPE Hydration Study

DSC of Hydrated DHPE. DSC heating curves of DHPE at different hydrations (0.0–30.0 wt % H_2O) are shown in Figure 1. At low hydration (≤10.0% H_2O), a single, broad endothermic transition was observed which decreased in temperature (enthalpy and entropy) from 95.2 °C [ΔH = 14.3 kcal/mol, ΔS = 38.7 cal/(mol·K)] to 78.8 °C [ΔH = 10.3 kcal/mol, ΔS = 29.3 cal/(mol·K)] (Figure 2). Above 10.0% H_2O, the DSC heating curve displayed two endothermic transitions which moved in opposite directions with increasing

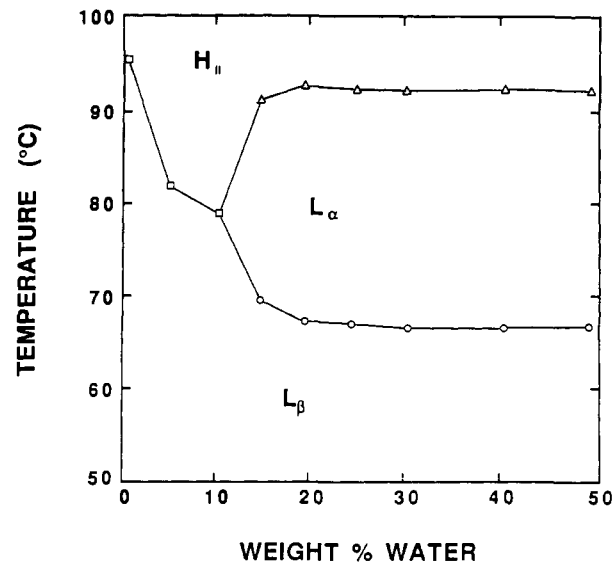

FIGURE 2: Transition temperature of the $L_\beta \rightarrow H_{II}$ transition (□), the $L_\beta \rightarrow L_\alpha$ transition (○), and the $L_\alpha \rightarrow H_{II}$ transition (△) of DHPE as a function of hydration.

hydration (Figures 1 and 2). The lower temperature, high-enthalpy, high-entropy (gel to liquid-crystalline, $L_\beta \rightarrow L_\alpha$) transition decreased in temperature with increasing hydration to 67.1 °C at 19.4% H_2O [ΔH = 7.7 kcal/mol, ΔS = 22.6 cal/(mol·K)]. The high-temperature, low-enthalpy, low-entropy (liquid-crystalline to inverted hexagonal, $L_\alpha \rightarrow H_{II}$) transition stabilized at 92.9 °C [ΔH = 1.83 kcal/mol, ΔS = 5.0 cal/(mol·K)] at the same hydration. The enthalpies and entropies for the $L_\beta \rightarrow L_\alpha$ chain-melting transition and the $L_\alpha \rightarrow H_{II}$ transition changed little above 20.0% H_2O [$L_\beta \rightarrow L_\alpha$, ΔH = 7.8–8.2 kcal/mol, ΔS = 23–24 cal/(mol·K); $L_\alpha \rightarrow H_{II}$, ΔH = 1.53 –1.89 kcal/mol, ΔS = 4.2–5.2 cal/(mol·K)]. Similar transition temperatures were observed for DHPE when run on a high-sensitivity calorimeter using a lipid concentration of 5.6 mg/mL at a much slower heating rate of 10 °C/h (data not shown).

X-ray Diffraction of Hydrated DHPE. X-ray diffraction patterns of DHPE at various hydrations were recorded in the gel phase (22 °C). A representative diffraction pattern of a DHPE sample at 25.0% H_2O and 22 °C is shown in Figure 3A. A series of lamellar reflections were observed corresponding to a bilayer repeat distance, d = 63.1 Å. The wide-angle region showed a sharp symmetric reflection at 1/4.18 $Å^{-1}$ indicating hexagonal packing of the alkyl chains. At 75 °C, a lamellar diffraction pattern was observed for DHPE at 50.0% H_2O (Figure 3B) with a diminished bilayer repeat of d = 49.2 Å using double-mirror optics. When recorded by using toroidal focusing geometry, a diffuse band located at 1/4.5 $Å^{-1}$ was visible, confirming the presence of a liquid-crystalline phase with melted alkyl chains at this temperature (data not shown). At 95 °C and 30.4% H_2O, three low-angle reflections were observed (Figure 3C) which indexed in the ratio 1:0.579:0.503, in very good agreement with the predicted ratio of $1:(1/\sqrt{3}):(1/\sqrt{4})$, and thus identified this as a hexagonal H_{II} phase. In addition, a direct gel to hexagonal phase transition ($L_\beta \rightarrow H_{II}$), with no intervening liquid-crystalline L_α phase, was observed for DHPE at a low hydration (10.2% H_2O) (data not shown).

The change in the bilayer periodicity of DHPE as a function of hydration at 22 °C is plotted in Figure 4, along with related structural parameters. DHPE at 22 °C exhibited a lamellar repeat distance (d) which increased with increasing hydration from 57.9 to 63.1 Å over the range 5.5% H_2O to 18.7% H_2O.

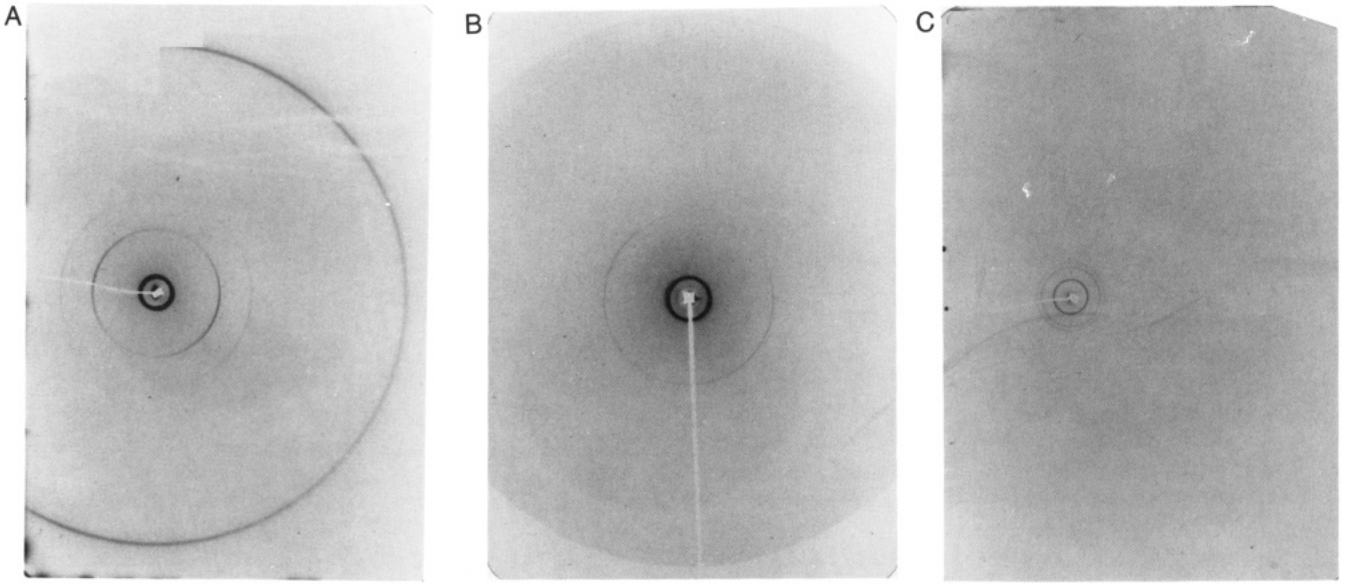

FIGURE 3: Representative X-ray diffraction patterns of hydrated DHPE, recorded by using double-mirror optics: (A) 25.0 wt % H_2O, T = 22 °C; (B) 50.0 wt % H_2O, T = 75 °C; (C) 30.4 wt % H_2O, T = 95 °C.

Above approximately 19% H_2O, the repeat distance (d) remained constant at 62.5 ± 0.9 Å (mean ± standard deviation). The lipid layer thickness (d_l), water layer thickness (d_w), and surface area per DHPE molecule at the lipid/water interface (S) were calculated according to Luzzati (1968), as described above, and by using the value for the partial specific volume of DHPE (ν_l = 0.943 mL/g) determined by Seddon et al. (1984). As presented in Figure 4, d_l decreases from 54.6 to 50.8 Å over the hydration range 5.5% H_2O to 18.7% H_2O. Meanwhile, d_w increases from 3.3 to 12.3 Å and S increases from 38.6 to 41.5 Å^2. Above the limiting hydration (~19% H_2O), the d spacing is essentially independent of water content; therefore, the calculated structural parameters are assumed to remain constant above 19% H_2O.

The intensities of the low-angle reflections for DHPE at different hydrations were analyzed to determine the changes in the structure amplitudes over the hydration range 5.5–21.5 wt % H_2O. This "swelling" study provided the phases of the structure amplitudes and has been applied previously to several phospholipid bilayer systems [for example, Torbet and Wilkins (1976), Janiak et al. (1979), McDaniel et al. (1983), McIntosh and Simon (1986), and Haas et al. (1990)]. Intensities were corrected for Lorentz and polarization factors [$I(h)*h^2$] and normalized with respect to each other. Normalized amplitudes plotted as a function of the reciprocal space s ($s = 2 \sin \theta/\lambda$) are shown in Figure 5A. The nodes are suggested by this plot and confirmed by use of the Shannon sampling theorem (Shannon, 1949; see also references for details). The derived phase sequence for n = 1–6 is –,+,–,–,+,– at all hydrations except for the sample containing 5.5% H_2O where a node was observed at n = 5. The corresponding electron density profiles, $\rho(X)$, were calculated and are displayed in Figure 5B. A trough of low electron density is seen at X = 0 Å for all hydrations and delineates the bilayer center. The two peaks at approximately ±25 Å define the location of the electron-rich phosphates of the head groups. Their separation (d_{p-p}) is another measure of bilayer thickness and suggests that this value ($d_{p-p} \simeq 50$ Å) changes only slightly (±2 Å) with changes in hydration (see also Figure 4).

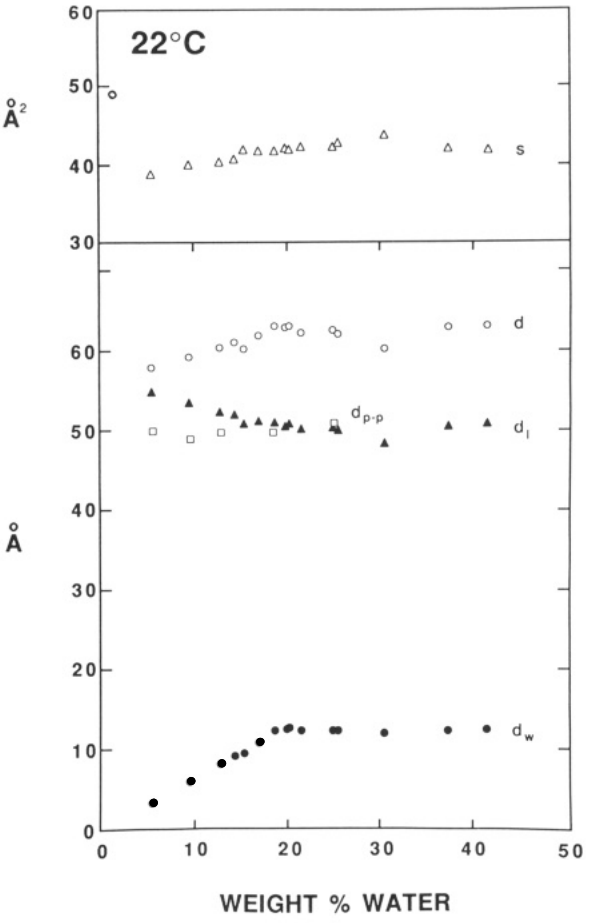

FIGURE 4: Bilayer structural parameters of DHPE as a function of water content at 22 °C. Bilayer periodicity, d (Å) (○); bilayer thickness, d_l (Å) (▲); water thickness, d_w (Å) (●); surface area per DHPE molecule at the lipid/water interface, S (Å^2) (△); phosphate–phosphate separation, d_{p-p} (Å) (□) from electron density profiles (see Figure 5B).

DHPE/DPPE Mixtures

DSC of Fully Hydrated DHPE/DPPE Mixtures. DHPE at full hydration exhibits two endothermic transitions by DSC (see Figure 6A): a low-temperature, high-enthalpy peak confirmed by X-ray diffraction data to be the $L_\beta \rightarrow L_\alpha$ transition and a high-temperature, low-enthalpy peak corresponding to the $L_\alpha \rightarrow H_{II}$ phase transition (see above). As DPPE is added to DHPE in excess water, the two transitions

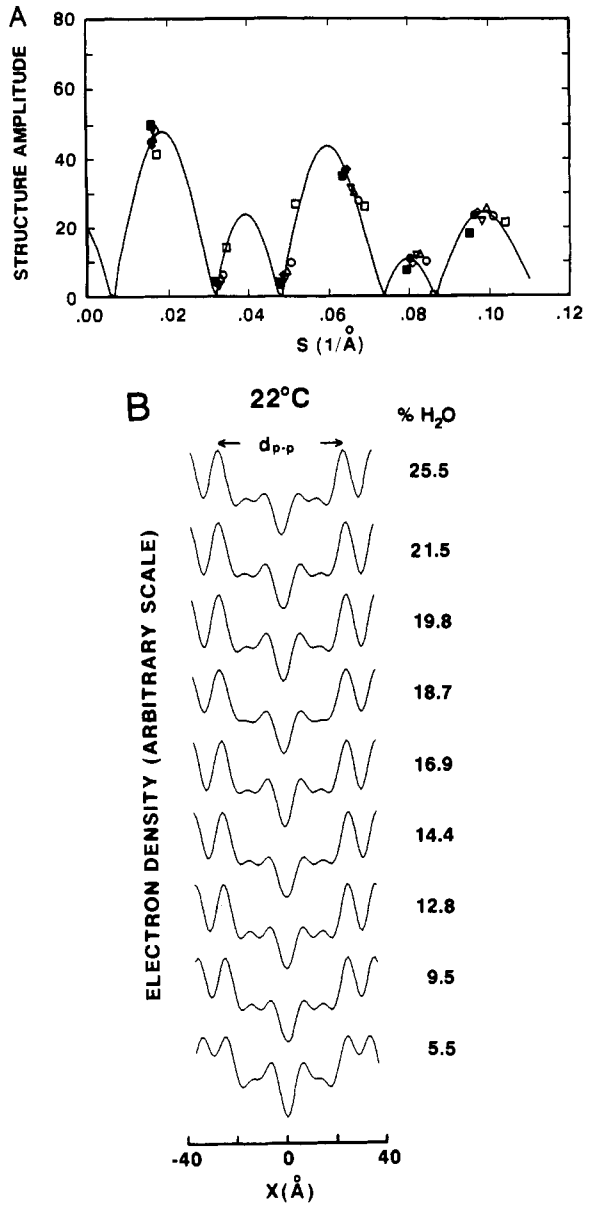

FIGURE 5: (A) Structure amplitudes of DHPE bilayers at 22 °C: 5.5 wt % H_2O (□); 9.5 wt % H_2O (○); 12.8 wt % H_2O (△); 14.4 wt % H_2O (▽); 16.9 wt % H_2O (◇); 18.7 wt % H_2O (■); 21.5 wt % H_2O (●). The continuous line is the amplitude curve for the 21.5 wt % H_2O data set calculated by using the Shannon sampling theory (see text). (B) Electron density profiles, $\rho(X)$, of DHPE at different hydrations at 22 °C.

move in opposite directions (see Figure 6A,B). The $L_\beta \rightarrow L_\alpha$ transition shows a small linear decrease as the mole percent of DPPE is increased, from 66.5 °C for fully hydrated DHPE to 63.5 °C for fully hydrated DPPE. A mixture containing 52.5 mol % DPPE and run on a high-sensitivity calorimeter (6.4 mg/mL, 10 °C/h) showed an $L_\beta \rightarrow L_\alpha$ transition occurring at a similar temperature as the same mixture at 50% H_2O run on the DSC-2 (data not shown). In contrast, the $L_\alpha \rightarrow H_{II}$ transition of DHPE/DPPE mixtures increases approximately linearly with increasing DPPE, from 86.3 °C at 0 mol % DPPE to 96.5 °C at 33.2 mol % DPPE. Above 33.2 mol % DPPE, the higher $L_\alpha \rightarrow H_{II}$ transition was not observed in the temperature range scanned (0–98 °C) and was presumed to occur above 98 °C in these mixtures. Extrapolation of the observed $L_\alpha \rightarrow H_{II}$ transition temperatures to greater amounts of DPPE gives a transition temperature for the $L_\alpha \rightarrow H_{II}$ transition of DPPE of 118 °C (see Figure 6B). This compares reasonably well with the value of 123 °C obtained by Seddon et al. (1983) for fully hydrated DPPE.

The enthalpy (expressed in calories per gram of total lipid) of the $L_\beta \rightarrow L_\alpha$ transition appears to be independent of the DHPE/DPPE molar ratio, at approximately 11.3 cal/g (data not shown). The enthalpy of the $L_\alpha \rightarrow H_{II}$ transition of DHPE determined here is ΔH = 1.4 cal/g. This enthalpy presumably decreases slightly, with increasing DPPE content (data not shown), to the enthalpy of the $L_\alpha \rightarrow H_{II}$ transition of pure DPPE, ΔH = 0.43 cal/g [determined by Seddon et al. (1983)]; however, an insufficient number of mixtures exhibiting an $L_\alpha \rightarrow H_{II}$ transition were obtained to enable us to detect with certainty the trend in the transition enthalpy with changing DHPE/DPPE molar ratio.

X-ray Diffraction of Fully Hydrated DHPE/DPPE Mixtures. Representative X-ray diffraction patterns of a mixture of DHPE and DPPE containing 10 mol % DPPE at 22, 75, and 95 °C are shown in panels A, B, and C, respectively, of Figure 7. At 22 °C (Figure 7A), a sharp symmetric reflection at 1/4.18 $Å^{-1}$, indicative of rigid hydrocarbon chains, and a lamellar diffraction pattern in the low-angle region, with d = 62.2 Å, indicate that this mixture is a bilayer in the gel state, L_β, at this temperature. At 75 °C (Figure 7B), the sharp reflection at 1/4.18 $Å^{-1}$ is replaced by a broad, diffuse band centered at 1/4.6 $Å^{-1}$ reflecting the loss of close packing of the hydrocarbon chains. A lamellar diffraction pattern is still observed in the low-angle region but with a reduced periodicity of d = 49.9 Å. Taken together, these data indicate the presence of a bilayer with melted chains, the liquid-crystalline L_α phase. When the temperature is raised to 95 °C (Figure 7C), the broad, diffuse band in the wide-angle region is still visible centered at 1/4.6 $Å^{-1}$, indicating that the hydrocarbon chains are still in the melted state. However, a lamellar diffraction pattern is no longer present. Instead, three reflections at low angle are observed which index in the ratio 1:0.587:0.5, in reasonable agreement with the ratio of $1:(1/\sqrt{3}):(1/\sqrt{4})$ which is considered diagnostic for a hexagonal H_{II} phase. Thus, the X-ray diffraction data along with the DSC data (Figure 6A) show that the mixture of 10 mol % DPPE in DHPE undergoes an $L_\beta \rightarrow L_\alpha$ transition at 68.1 °C (ΔH = 11.5 cal/g) and an $L_\alpha \rightarrow H_{II}$ transition at 89.8 °C (ΔH = 1.3 cal/g).

The measured d spacing for a number of DHPE/DPPE mixtures at 22 °C remains essentially constant at 62.1 ± 0.4 Å (data not shown). The bilayer periodicity of DHPE/DPPE mixtures in the L_α phase at 75 °C increases only slightly from 49.9 Å at 0 mol % DPPE to 51.8 Å at 100 mol % DPPE in an approximately linear fashion (data not shown). Measurements of the wide-angle reflections above and below the main transition of several mixtures reveal a sharp reflection at approximately 1/4.15 $Å^{-1}$ at 22 °C which becomes a broad diffuse band centered at 1/4.6 $Å^{-1}$ at 75 °C, denoting chain melting as with hydrated DHPE samples.

Discussion

In this study, we examined the contributions of the phospholipid head group and the linkage of the hydrocarbon chains to thermotropic behavior as well as their effects on structure. This was done by examining DHPE, the ethanolamine counterpart of DHPC, alone and in mixtures with the corresponding ester phosphatidylethanolamine, DPPE.

Ether-linked phosphatidylcholines (PCs), mixtures of ether- and ester-linked PCs, and PCs containing both an ether and an ester linkage on the same molecule can all form interdigitated bilayers in the gel phase (Kim et al., 1987a,b; Laggner et al., 1987; Lohner et al., 1987; Haas et al., 1990). In contrast, X-ray diffraction data shown here clearly demonstrate

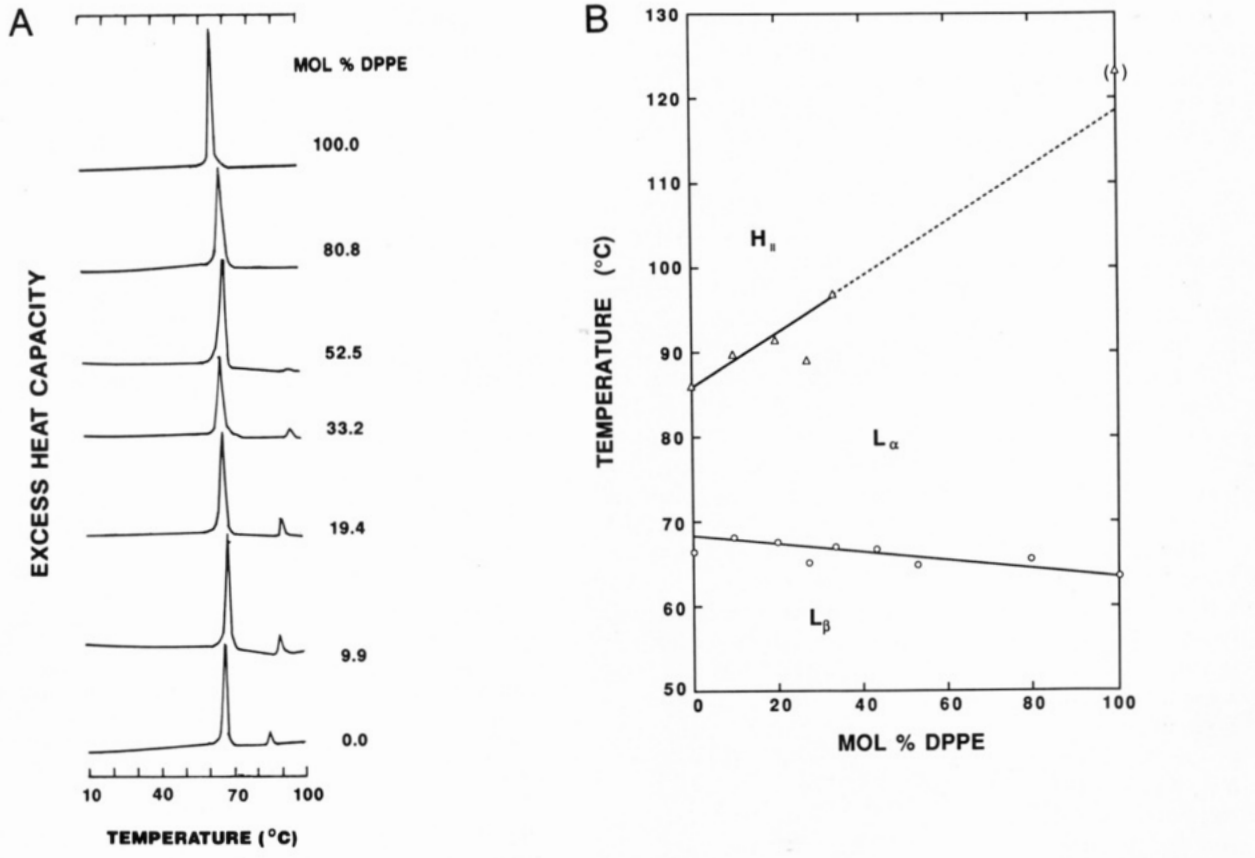

FIGURE 6: (A) Representative DSC heating curves of fully hydrated (50 wt % H_2O) DHPE/DPPE mixtures. (B) Transition temperatures (degrees centigrade) of $L_\beta \rightarrow L_\alpha$ (○) and $L_\alpha \rightarrow H_{II}$ (△); data shown in parentheses were obtained from Seddon et al. (1983).

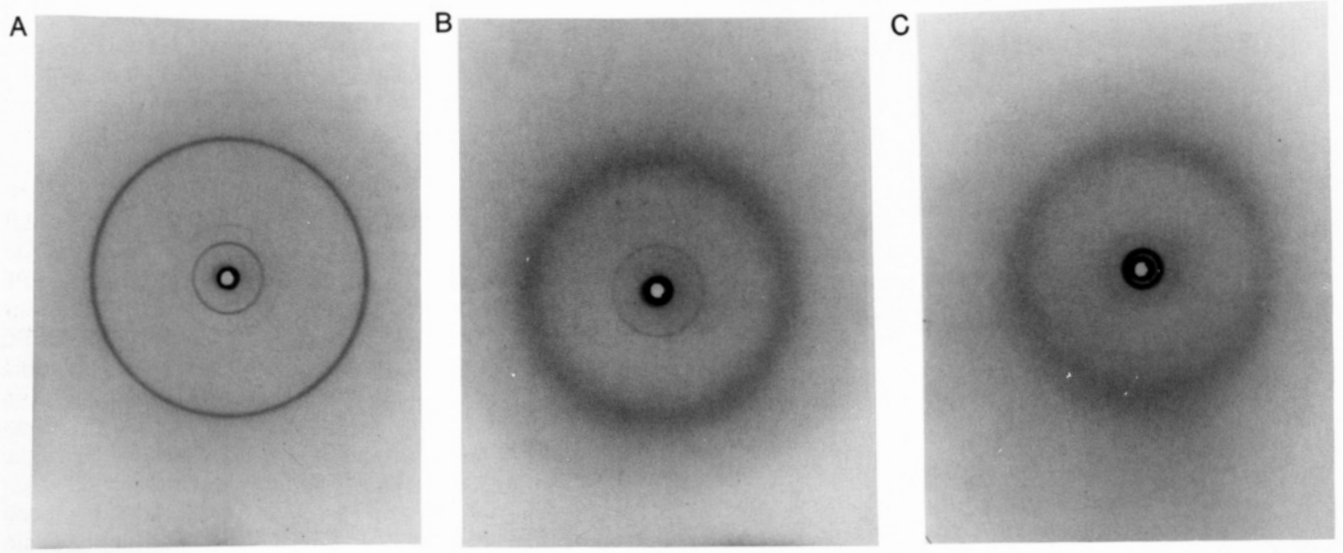

FIGURE 7: Representative X-ray diffraction patterns of a fully hydrated DHPE/DPPE mixture (50 wt % H_2O) containing 10 mol % DPPE, recorded by using toroidal optics: (A) 22 °C; (B) 75 °C; (C) 95 °C.

that DHPE is in a noninterdigitated form both above and below the chain-melting phase transition at all hydrations. The inverted hexagonal phase (H_{II}) is also seen in DHPE but not in DHPC, suggesting that both head group and chain linkage contribute in some way to form the observed structures.

Calorimetric evidence shows that the $L_\alpha \rightarrow H_{II}$ phase transition temperature decreases with decreasing hydration while just the opposite occurs for the $L_\beta \rightarrow L_\alpha$ phase transition (Figures 1 and 2). Therefore, it appears that lower water contents destabilize the L_α phase and stabilize both the L_β and H_{II} phases until at very low hydration ($\sim$10 wt % H_2O) the L_β phase converts directly to the H_{II} phase. A direct $L_\beta \rightarrow H_{II}$ phase transition has previously been demonstrated to occur in a mixture of DPPC and palmitic acid at low pH and in distearoylphosphatidylethanolamine (DSPE), in saturated NaCl (Marsh & Seddon, 1982). It has also been observed in DHPE alone (Caffrey, 1985), as well as in saturated NaCl (Marsh & Seddon, 1982). The phase diagram which has been constructed for DHPE in combination with water is in basic agreement with the findings of Seddon et al. (1983) for other PEs, and also with the studies of Caffrey (1985) for hydrated DHPE. Above the limiting hydration of 19 wt % H_2O, DSC reveals little change occurring in the transition temperatures, ΔH, or ΔS of the phase transitions of DHPE with increasing

hydration. Therefore, above the limiting hydration, the structure remains stable. For the L_β phase, the X-ray diffraction data support this conslusion since above 19 wt % H_2O (8.6 mol of water/mol of DHPE) the d spacing is found to remain approximately constant at 62 Å.

The calculated values of d_l and d_w for the L_β phase at 22 °C (Figure 4) show that the initial increase in the d spacing is due to an increase in the thickness of the water layer. At low hydration, d_l is seen to decrease with increasing water content up to the limiting hydration. It is not known, however, whether this reflects a real decrease in the lipid bilayer (since the calculation assumes that there is no overlap of d_l and d_w). This trend is, however, seen in other lipid systems [see, for example, Janiak et al. (1979) and Kim et al. (1987a)]. The values for S change relatively little with increasing hydration. PC bilayers, on the other hand, which have a greater hydration capacity, show a larger change in surface area (S) over their more extended hydration range (Janiak et al., 1979; Kim et al., 1987a; Haas et al., 1990). The values of S are also higher for DHPC in a noninterdigitated gel phase bilayer than for DHPE in a similar state which likely reflects the larger head group of PCs such that a larger surface area is required to accommodate it. Similarly, an interdigitated bilayer shows a greatly increased surface area, $S \simeq 75$ Å^2, as a consequence of the added volume of the hydrocarbon chains from the opposite side of the bilayer (Kim et al., 1987a). The value for S above the limiting hydration of DHPE in the gel phase, calculated here ($S = 42.1 \pm 0.6$ Å^2), is identical with that obtained by Seddon et al. (1984) for gel phase didodecylphosphatidylethanolamine (DDPE) but is less than that of diarachidonylphosphatidylethanolamine (DAPE) ($S = 46.8$ Å^2), also in the gel phase. This difference is likely due to the significant tilt of the hydrocarbon chains of DAPE with respect to the bilayer normal whereas the hydrocarbon chains of DDPE are approximately parallel with the bilayer normal (Seddon et al., 1984). The hydrocarbon chains of DHPE in the gel state are also approximately parallel to the bilayer normal as evidenced by the sharp symmetric reflection in the X-ray diffraction pattern at 1/4.18 Å, and the fact that the calculated surface area S (Figure 4) is approximately twice the cross-sectional area of a single hydrocarbon chain (20 Å^2). Consequently, factors such as chain tilt, head-group size, and chain interdigitation all influence the surface area per lipid molecule.

Electron density profiles appear as expected (Figure 5B) and show a trough in the center of a bilayer which clearly indicates a noninterdigitated bilayer structure. One does not expect a trough in the electron density profile to occur in the center of the bilayer in an interdigitated structure due to overlap of the hydrocarbon chains from opposite sides of the bilayer [see Kim et al. (1987a)]. Two peaks corresponding to the phosphate groups on opposite sides of the bilayer are also observed. The values of d_{p-p} agree well with d_l above 19% H_2O even though they measure different structural parameters. Diffraction patterns were not systematically recorded in the L_α and H_{II} phases because of the high temperature of the $L_\alpha \rightarrow H_{II}$ transition; therefore, the change in the structural parameters with hydration was not followed in these phases. The structural changes of DHPE with temperature and hydration are summarized in Figure 8.

In mixtures of DHPE and DPPE, the temperature of the $L_\beta \rightarrow L_\alpha$ phase transition increases slightly while the $L_\alpha \rightarrow H_{II}$ transition temperature decreases much more with increasing amounts of DHPE (Figure 6B), both changes occurring in a reasonably linear fashion. The implication is that

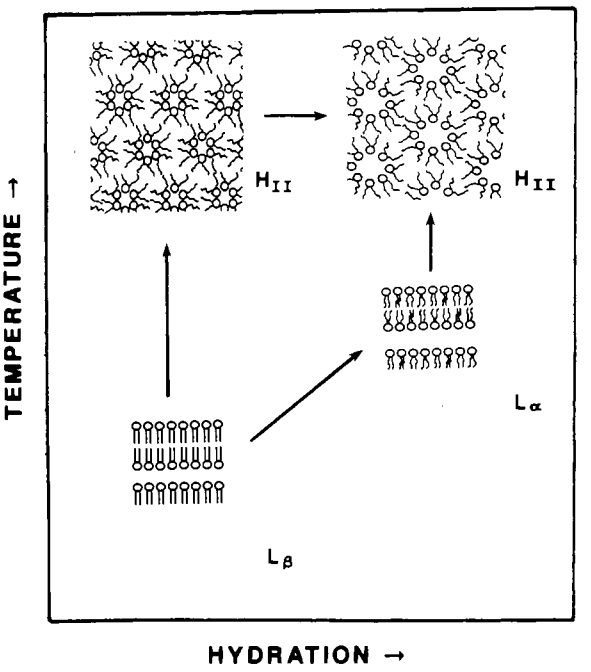

FIGURE 8: Structural representation of the hydration- and temperature-dependent transitions of DHPE. At low hydrations, a direct and reversible $L_\beta \rightarrow H_{II}$ transition is observed. At approximately 15 wt % H_2O and above, an intermediate L_α phase occurs, $L_\beta \rightarrow L_\alpha \rightarrow H_{II}$.

the ether linkage is stabilizing both the L_β and H_{II} phases at the expense of the L_α phase. These results are consistent with the findings of Seddon et al. (1984), who found that perturbations of PEs (e.g., chain length, salt concentration) caused opposite changes in the temperatures of their $L_\beta \rightarrow L_\alpha$ and $L_\alpha \rightarrow H_{II}$ phase transitions. This is not always the case, however, and the transition temperatures may shift in the same direction (Epand et al., 1988). The transition temperatures change approximately linearly from the corresponding transition temperatures in pure DPPE, suggesting complete miscibility of DHPE and DPPE in all three phases (L_β, L_α, H_{II}). The X-ray diffraction data also argue for the existence of a single phase in DHPE/DPPE mixtures since only one phase could be observed in X-ray diffraction patterns of DHPE/DPPE mixtures at the temperatures at which diffraction patterns were recorded. Since DHPE and DPPE both exhibit identical phases, the lack of eutectic behavior in the gel phase as observed for DHPC/DPPC mixtures (Kim et al., 1987b) is not surprising. [Unlike DHPC, DPPC does not form an interdigitated bilayer under normal conditions, although one will form at high pressures (Braganza & Worcester, 1986).] An idealized phase diagram of the DHPE/DPPE system, reflecting the DSC and X-ray diffraction data, is presented in Figure 9.

The formation of the H_{II} phase in lipids is often explained in terms of the average shape of the lipid molecule. Cylindrically shaped molecules will tend to form lamellar structures while molecules with greater hydrocarbon regions relative to the polar head group form inverted cones and prefer the H_{II} phase (Israelachvili et al., 1980; Cullis et al., 1983). Boggs et al. (1981) have postulated that the ether-linked lipids are closer packed than the ester-linked lipids, and this promotes more extensive hydrogen bonding between lipid molecules, especially in the head-group region. Consequently, the more extensive intermolecular interactions of the ether-linked PE serve to stabilize the H_{II} and L_β phases and destabilize the L_α phase. As illustrated by the mixed DHPE/DPPE system, the ether linkage affects the $L_\alpha \rightarrow H_{II}$ phase transition temperature

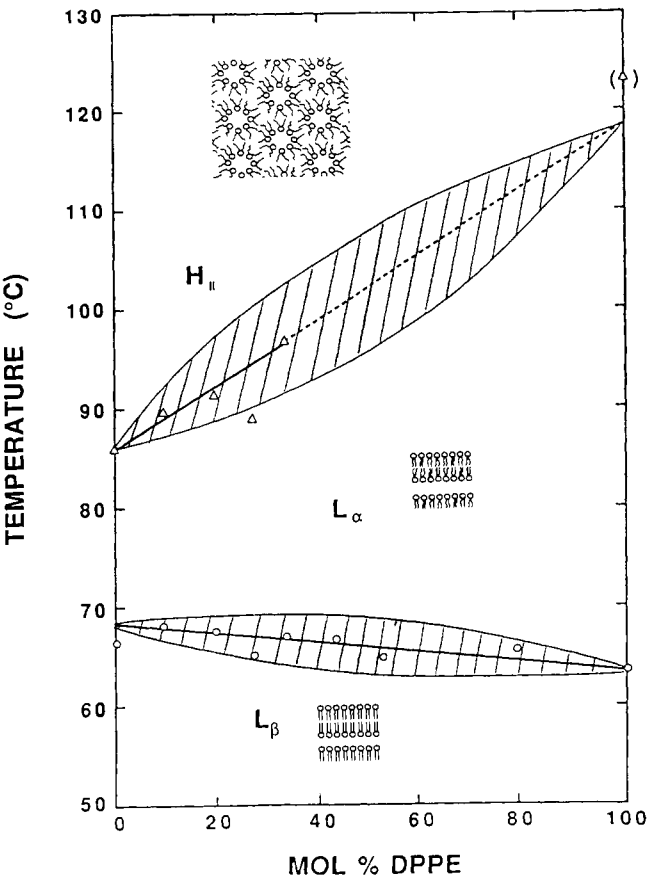

FIGURE 9: Idealized phase diagram of the DHPE/DPPE system at full hydration based on DSC and X-ray diffraction data. Onset and completion temperatures are not accurately determined from DSC experiments due to heating rate effects, etc.

more than the $L_\beta \rightarrow L_\alpha$ transition temperature (see Figures 6B and 9).

Alternatively, the H_{II} phase has been viewed as a balance of opposing forces. On the one hand is the tendency of a lipid monolayer to curl with an intrinsic radius of curvature specific to that lipid. On the other hand, there are the hydrocarbon packing constraints which tend to favor the lamellar structure because of its less stringent chain packing requirements (Gruner, 1985; Tate & Gruner, 1987). The intrinsic radius of a lipid is affected by, among other things, the polar head group, the hydrocarbon chain length, and the hydrocarbon chain linkage (Seddon et al., 1983, 1984). Following this line of reasoning, it would seem that the ethanolamine head group has decreased the intrinsic radius of curvature, allowing DHPE to form the H_{II} phase while DHPC does not. Likewise, the ether linkage appears to increase the tendency of the lipid to curl when compared with the ester linkage.

Conclusions

DHPE and DPPE at full hydration appear to be completely miscible in all proportions in the three phases, L_β, L_α, and H_{II}, whereas DPPC can only be accommodated into interdigitated DHPC gel phase bilayers to approximately 30 mol % DPPC. DHPE bilayers are noninterdigitated; therefore, both the choline head group and ether linkage are necessary for interdigitation to occur. Substitution of ethanolamine for the choline group abolishes chain interdigitation and favors the formation of the H_{II} phase. Of interest is the possibility that mixtures of DHPE and DHPC are able to form either an interdigitated or an H_{II} phase. One expects that DHPE would hinder formation of an interdigitated bilayer in DHPC at high concentrations, while DHPC would in turn destabilize the H_{II} phase of DHPE. These predictions are currently being tested.

Acknowledgments

We thank Neil Haas for useful discussions and Dr. David Atkinson for technical advice.

Registry No. DHPE, 54285-60-8; DPPE, 3026-45-7.

References

Boggs, J. M., Stamp, D., Hughes, D. W., & Deber, C. M. (1981) *Biochemistry 20*, 5728–5735.

Braganza, L. F., & Worcester, D. L. (1986) *Biochemistry 25*, 2591–2596.

Caffrey, M. (1985) *Biochemistry 24*, 4826–4844.

Chapman, D., Byrne, P., & Shipley, G. G. (1966) *Proc. R. Soc.* London, A *290*, 115–142.

Cullis, P. R., deKruijff, B., Hope, M. J., Verkleij, A. J., Nayer, R., Tilcock, C. P. S., Madden, T. D., & Bally, M. B. (1983) in *Membrane Fluidity in Biology* (Aloia, R. C., Ed.) Vol. 1, pp 39–81, Academic Press, New York.

Elliott, A. J. (1965) *J. Sci. Instrum. 42*, 312–316.

Epand, R. M., Epand, R. F., & Lancaster, C. R. D. (1988) *Biochim. Biophys. Acta 945*, 161–166.

Franks, A. (1958) *Br. J. Appl. Phys. 9*, 349–352.

Goldfine, H., Johnston, N. C., Mattai, J., & Shipley, G. G. (1987) *Biochemistry 26*, 2814–2822.

Gruner, S. M. (1985) *Proc. Natl. Acad. Sci. U.S.A. 82*, 3665–3669.

Haas, N. S., Sripada, P. K., & Shipley, G. G. (1990) *Biophys. J. 57*, 117–124.

Hauser, H., Paltauf, F., & Shipley, G. G. (1982) *Biochemistry 21*, 1061–1067.

Hing, F. S., & Shipley, G. G. (1991) *FASEB J. 5*, A1155.

Hitchcock, P., Mason, R., Thomas, K. M., & Shipley, G. G. (1974) *Proc. Natl. Acad. Sci. U.S.A. 71*, 3036–3040.

Israelachvili, J. N., Marcelja, S., & Horn, R. G. (1980) *Q. Rev. Biophys. 13*, 121–200.

Janiak, M. J., Small, D. M., & Shipley, G. G. (1976) *Biochemistry 15*, 4575–4580.

Janiak, M. J., Small, D. M., & Shipley, G. G. (1979) *J. Biol. Chem. 254*, 6068–6078.

Kim, J. T., Mattai, J., & Shipley, G. G. (1987a) *Biochemistry 26*, 6592–6598.

Kim, J. T., Mattai, J., & Shipley, G. G. (1987b) *Biochemistry 26*, 6599–6603.

Laggner, P., Lohner, K., Degovics, G., Muller, K., & Schuster, A. (1987) *Chem. Phys. Lipids 44*, 31–60.

Lohner, K., Schuster, A., Degovics, G., Muller, K., & Laggner, P. (1987) *Chem. Phys. Lipids 44*, 61–70.

Luzzatti, V. (1968) in *Biological Membranes* (Chapman, D., Ed.) pp 71–123, Academic Press, London and New York.

Marsh, D., & Seddon, J. M. (1982) *Biochim. Biophys. Acta 690*, 117–123.

Mattai, J., Sripada, P. K., & Shipley, G. G. (1987) *Biochemistry 26*, 3287–3297.

McDaniel, R. V., McIntosh, T. J., & Simon, S. A. (1983) *Biochim. Biophys. Acta 731*, 97–108.

McIntosh, T. J., & Simon, S. A. (1986) *Biochemistry 25*, 4058–4066.

Mulukutla, S., & Shipley, G. G. (1984) *Biochemistry 23*, 2514–2519.

Ruocco, M. J., & Shipley, G. G. (1982a) *Biochim. Biophys. Acta 691*, 309–320.

Ruocco, M. J., & Shipley, G. G. (1982b) *Biochim. Biophys. Acta 684*, 59–66.

Ruocco, M. J., Siminovitch, D. J., & Griffin, R. G. (1985) *Biochemistry 24*, 2406–2411.
Seddon, J. M., Cevc, G., & Marsh, D. (1983) *Biochemistry 22*, 1280–1289.
Seddon, J. M., Cevc, G., Kaye, R. D., & Marsh, D. (1984) *Biochemistry 23*, 2634–2644.
Serrallach, E. N., Dijkman, R., De Haas, G. H., & Shipley, G. G. (1983) *J. Mol. Biol. 170*, 155–174.
Shah, J., Sripada, P. K., & Shipley, G. G. (1990) *Biochemistry 29*, 4254–4262.
Shannon, C. E. (1949) *Proc. Inst. Radio. Eng. N.Y. 37*, 10–21.
Snyder, F. (1985) in *Biochemistry of Lipids and Membranes* (Vance, D. E., & Vance, J. E., Eds.) pp 271–298, Benjamin/Cummings, Menlo Park, CA.
Tate, M. W., & Gruner, S. M. (1987) *Biochemistry 26*, 231–236.
Torbet, J., & Wilkins, M. H. F. (1976) *J. Theor. Biol. 62*, 447–458.
Wieslander, Å., Christiansson, A., Rilfors, L., & Lindblom, G. (1980) *Biochemistry 19*, 3650–3655.
Wieslander, Å., Christiansson, A., Rilfors, L., Khan, A., Johansson, L. B.-Å., & Lindblom, G. (1981a) *FEBS Lett. 124*, 273–278.
Wieslander, Å., Rilfors L., Johansson, L. B.-Å., & Lindblom, G. (1981b) *Biochemistry 20*, 730–735.

Correlation of Gene and Protein Structure of Rat and Human Lipocortin I†

Roger T. Kovacic, Richard Tizard, Richard L. Cate, Alexis Z. Frey, and Barbara P. Wallner*
Biogen Inc., 14 Cambridge Center, Cambridge, Massachusetts 02142
Received April 12, 1991; Revised Manuscript Received July 1, 1991

ABSTRACT: Lipocortins (annexins) are a family of calcium-dependent phospholipid-binding proteins with phospholipase A_2 inhibitory activity. The characteristic primary structure of members of this family consists of a core structure of four or eight repeated domains, which have been implicated in calcium-dependent phospholipid binding. In two lipocortins (I and II) a short amino-terminal sequence distinct from the core structure has potential regulatory functions which are dependent on its phosphorylation state. We have isolated the rat and the human lipocortin I genes and found that they both consist of 13 exons with a striking conservation of their exon–intron structure and their promoter and amino acid sequences. Both lipocortin I genes are at least 19 kbp in length with exons ranging from 57 to 123 bp interrupted by introns as large as 5 kbp. Each of the four repeat units of lipocortin I are encoded by two consecutive exons while individual exons code for the highly conserved putative calcium-binding domains. The promoter sequences in the rat and in human genes are highly conserved and contain nucleotide sequences characterized as enhancer sequences in other genes. The structure of the lipocortin I gene lends support to the hypothesis that the lipocortin genes arose by a duplication of a single domain.

Lipocortins (lately also referred to as annexins) are a group of calcium/phospholipid-binding proteins with phospholipase A_2 (PLA_2) inhibitory activity. Originally characterized as dexamethasone-induced inhibitors of eicosanoid production [for review, see Flower (1985, 1988)], members of the lipocortin family are now implicated in the regulation of a variety of biological events, such as blood coagulation and differentiation, and in various aspects of the immune response and inflammation (Maurer-Fogy et al., 1988; Funakoshi et al., 1987; Cirino & Flower, 1987a,b; Cirino et al., 1989; Ishizaka, 1985).

Lipocortin-like proteins have also been isolated by other groups on the basis of their calcium-dependent phospholipid-binding properties and have been given other names, including p35 (Fava & Cohen, 1984), p36 (Gerke & Weber, 1985), calpactins (Glenney, 1986), endonexins and p68 (Davies & Crumpton, 1985; Gerke & Weber, 1984), annexins (Geisow et al., 1987), calcimedins (Mathew et al., 1986), calelectrins (Geisow, 1986a), chromobindins (Creutz et al., 1987), and proteins I–III (Weber et al., 1987; Shadle et al., 1985; Burns et al., 1989) [for reviews, see Klee (1988), Flower (1988), and Wallner (1989)]. Eight distinct members of the mammalian lipocortin family have now been identified (Pepinsky et al., 1988; Haigler et al., 1989; Hauptman et al., 1989). The amino acid sequences of the lipocortins are highly conserved between species with all members showing 40–50% sequence homology to each other.

Lipocortins I and II appear to play a role in signal transduction: lipocortin I in EGF-dependent cellular proliferation and lipocortin II in oncogenic transformation. Lipocortin I (p35, calpactin II) is the major physiologic substrate of the EGF-induced EGF receptor kinase (Pepinsky & Sinclair, 1986; Sawyer & Cohen, 1985), and lipocortin II (p36, calpactin I) is identical with the major substrate of viral and growth factor dependent protein kinases (Huang et al., 1986; Erikson & Erikson, 1980; Saris et al., 1986).

The characteristic structure of lipocortin-like proteins consists of a 4-fold repeated domain of 70 amino acids (Wallner et al., 1986; Kretsinger & Creutz, 1986; Geisow, 1986b; Weber & Johnsson, 1986). Lipocortin I interacts with cellular membranes and vesicles in a calcium-dependent manner. A highly conserved region of 14 amino acids within each repeat unit has been implicated as the calcium-binding site (Weber & Johnsson, 1986; Schlaepfer & Haigler, 1987). The structure of this putative calcium-binding site is different from the EF-hand structure of other calcium-binding proteins.

† The genetic sequence in this paper has been submitted to GenBank under Accession Number J05339.
* Author to whom correspondence should be addressed.

0006-2960/91/0430-9015$02.50/0 © 1991 American Chemical Society